

Supporting Information

Pioneering Nucleation for Stable Ultraviolet to Deep Blue Illuminating Two-Dimensional Perovskite Nanoplates by using Saturated Salt Solution

Anupriya Singh,¹ Yi-Chia Chen,^{1*} Kuan-Chang Wu,² Yu-Ying Shih,¹ Tzu-Chi Huang,³ Wei-Lon Wei,⁴ Yu-Dian Chen,² Priyadarshini HN,² Jou-Chun Lin,¹ Bi-Hsuan Lin,⁴ Mau-Tsu Tang,⁴ Di-Yan Wang^{1*}

¹ Department of Chemistry, National Taiwan Normal University, Taipei, 11677, Taiwan

² Department of Chemistry, Tunghai University, Taichung 40704, Taiwan.

³ Department of Materials Science and Engineering, National Tsing Hua University, Hsinchu 30013, Taiwan

⁴ National Synchrotron Radiation Research Center, Hsinchu 300092, Taiwan

Corresponding author: diyanwang@ntnu.edu.tw; yichia899@gmail.com

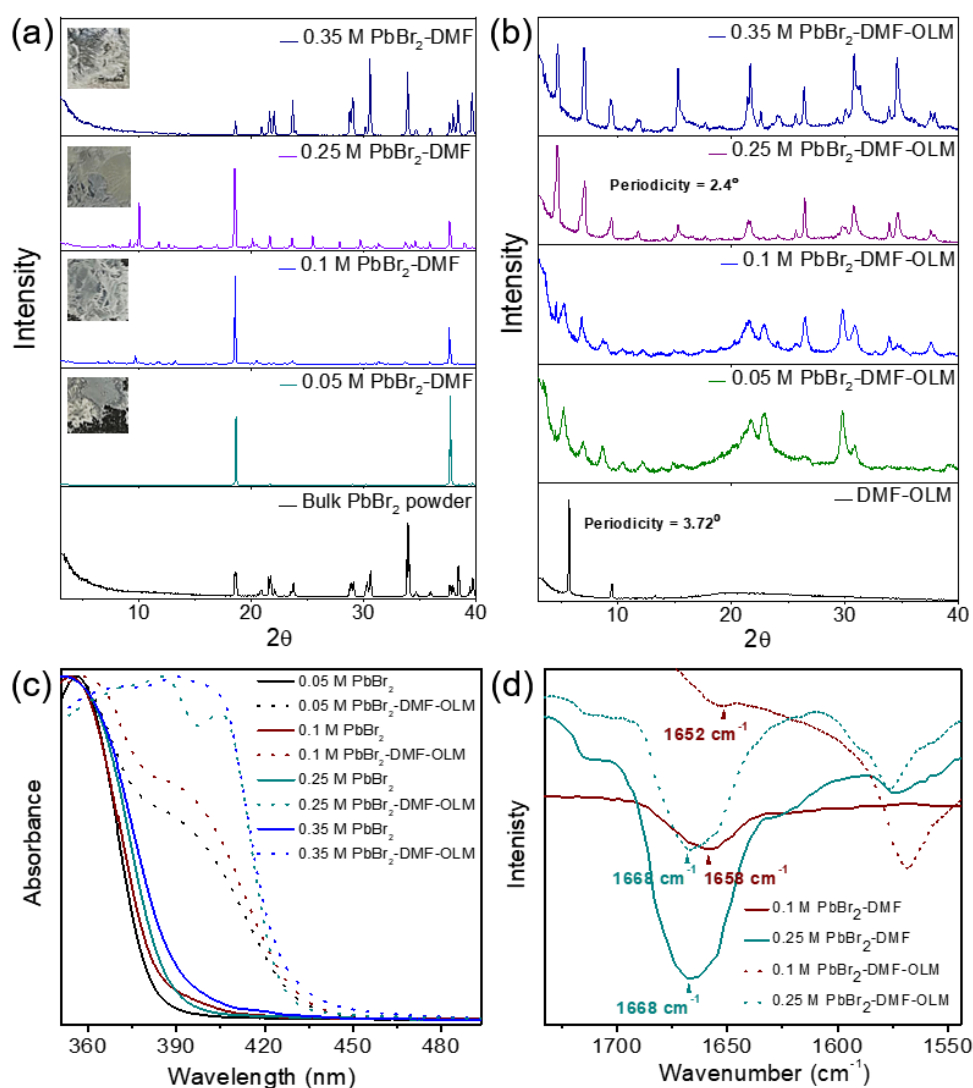


Figure S1. (a) X-ray diffraction patterns for the films made of variable amounts of PbBr₂ in DMF. (b) the effect of OLM addition on XRD patterns of (a). (c) UV-Vis absorption spectra for films made of variable amounts of PbBr₂ and PbBr₂-OLM in DMF. (d) Fourier transform infrared spectroscopic curves for variable amounts of PbBr₂-DMF and PbBr₂-DMF-OLM.

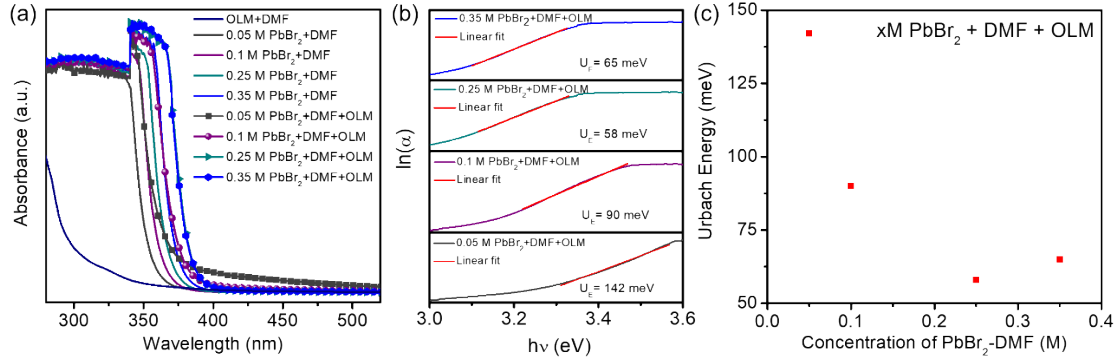


Figure S2. (a) UV-Vis absorption spectra for variable molar concentration of PbBr₂ in DMF. (b) Urbach energy (U_E) calculations for the band-edge slope of the absorption spectrum signify the reduction of defect density for higher molar concentrations. (c) The plot of Urbach energy against the variable molar concentration of PbBr₂ in DMF corresponds to (b).

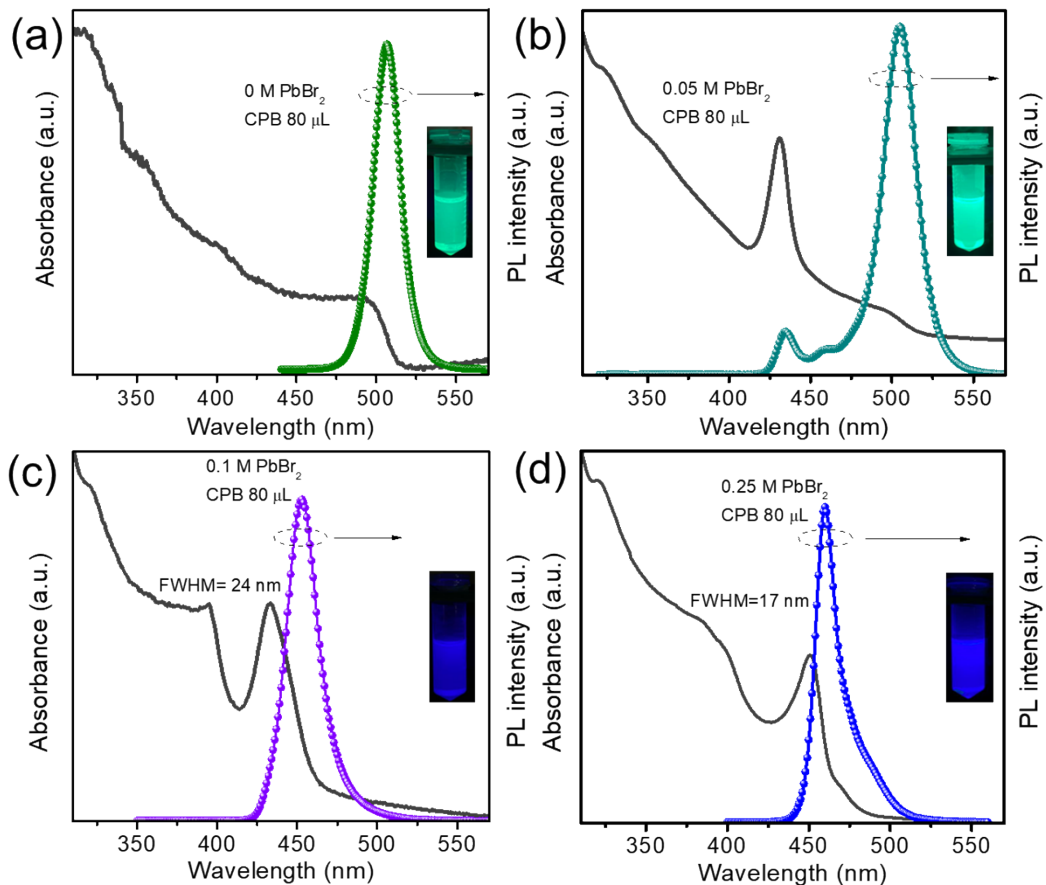


Figure S3. Normalized UV-Vis absorption spectrum with photoluminescence spectrum displaying the tuning of the band-edge and emission peak achieved by using a consistent amount of CPB solution (80 μL) while varying the concentration of PbBr₂: (a) no excess PbBr₂, (b) 0.05 M PbBr₂, (c) 0.1 M PbBr₂, (d) 0.25 M PbBr₂.

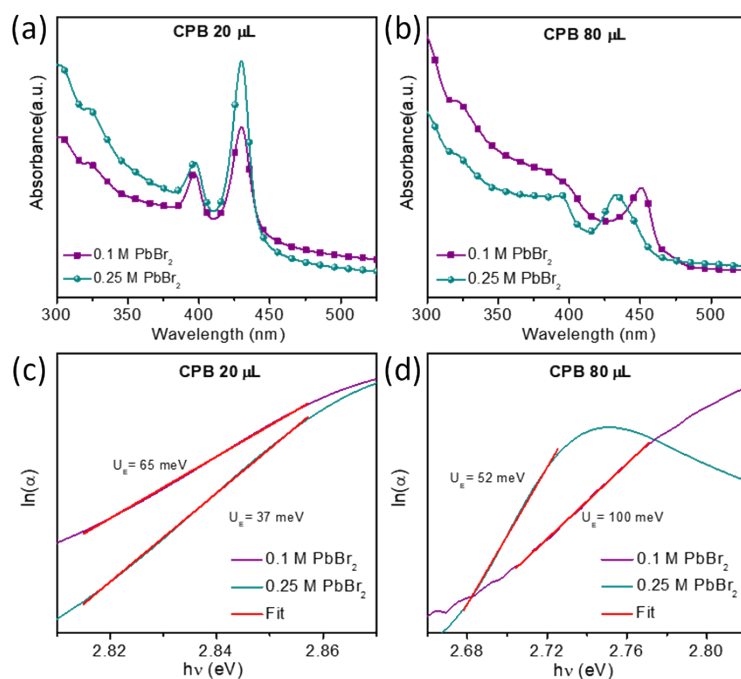


Figure S4. Comparison of normalized absorbance for nanoplates formed from 0.1 M and 0.25 M PbBr_2 base solution for (a) CPB = 20 μL i.e., for $n=2$, (b) CPB = 80 μL i.e., for $n=3$; Urbach energy calculations for the respective absorption band edges signifying a reduction in defect states for NCs from 0.25 M PbBr_2 base solution for (c) CPB = 20 μL i.e., for $n=2$, (d) CPB = 80 μL i.e., for $n=3$.

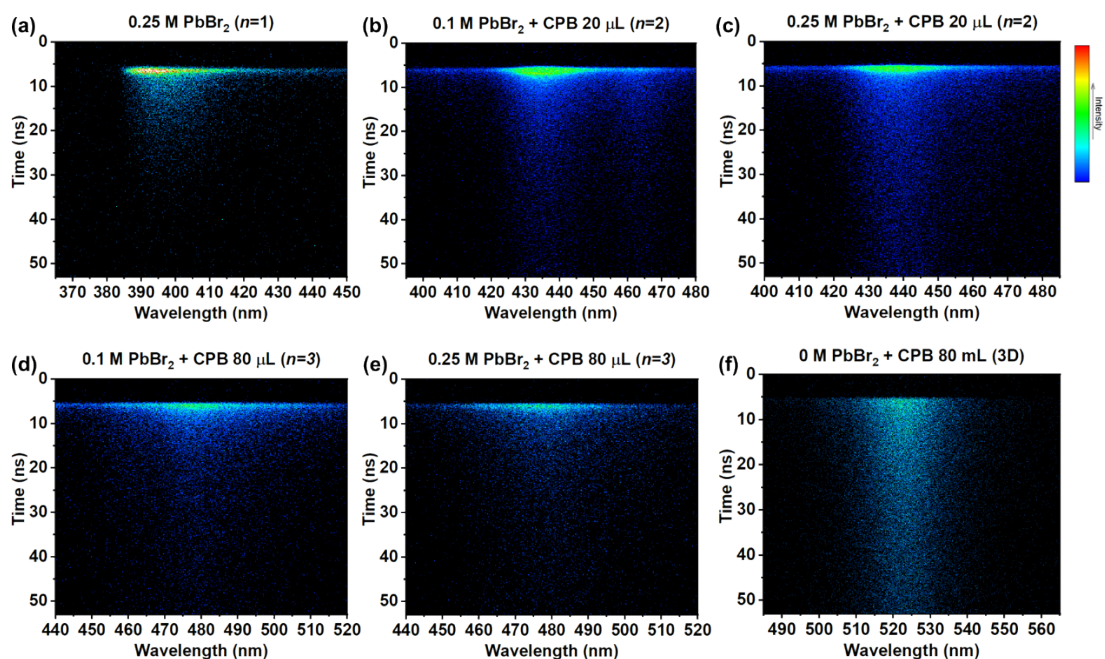


Figure S5. Streak camera images of 2D $n=1, 2, 3$, and 3D perovskite nanomaterials were recorded under 375 nm laser excitation.

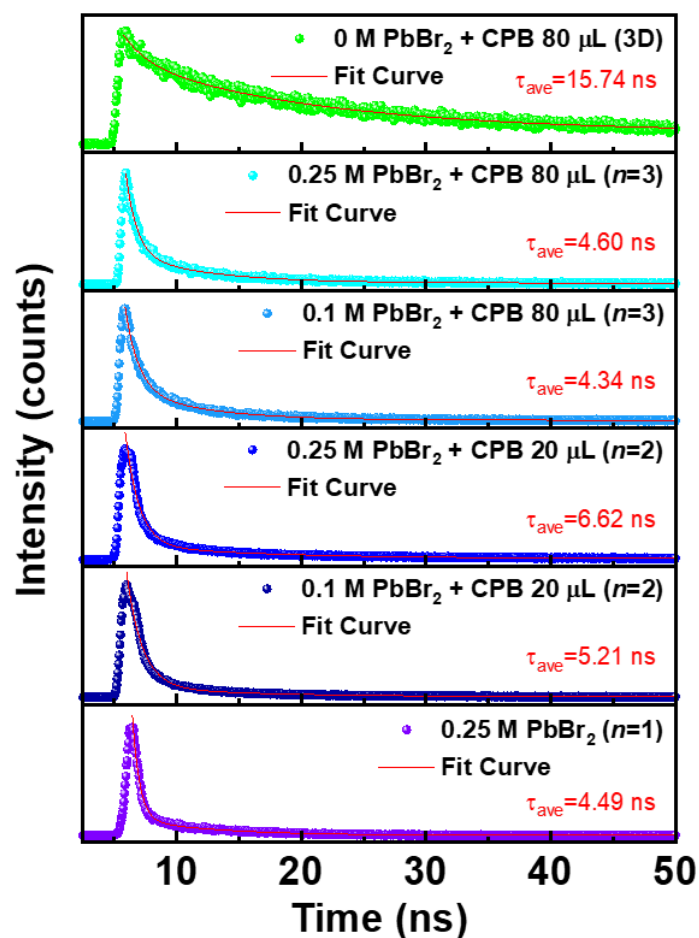


Figure S6. Time-resolved photoluminescence (TRPL) spectra of 2D $n=1, 2, 3$, and 3D perovskite nanomaterials, extracted from the streak camera images from Figure S5. The TRPL decay curves were fitted by the bi-exponential decay function.

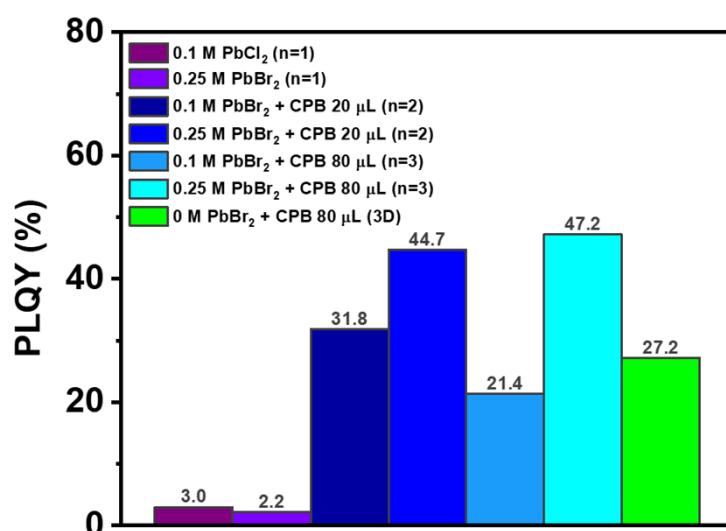


Figure S7. The PLQY results of 2D ($n=1, 2, 3$) and 3D perovskite nanomaterials synthesized using a LARP method.

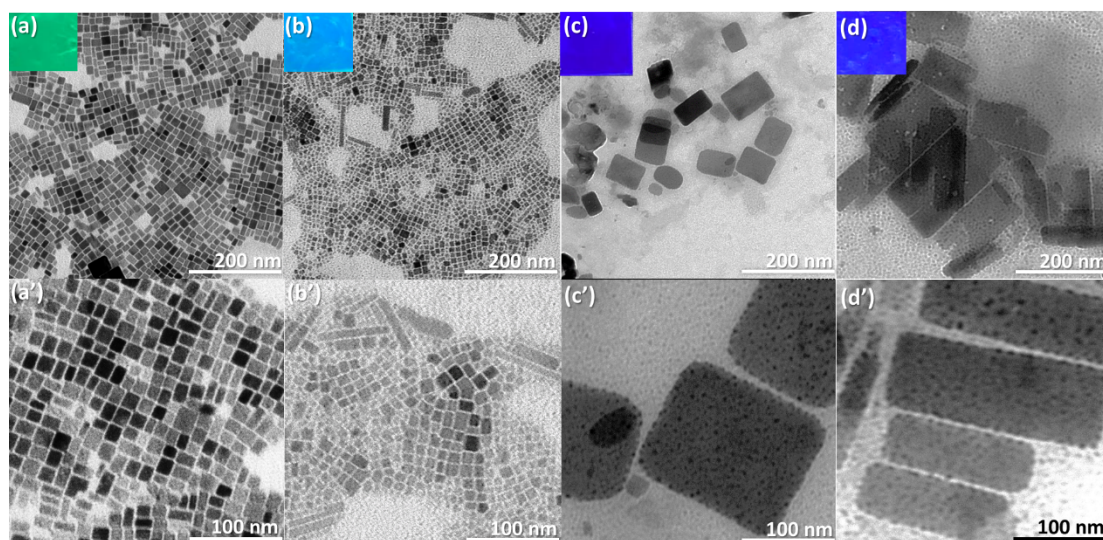


Figure S8. HRTEM images of perovskite nanostructures in (a) 0 M PbBr₂, (b) 0.05 M PbBr₂, (c) 0.1 M PbBr₂, and (d) 0.25 M PbBr₂ systems. (a'-d') Zoomed images of the figure (a-d), respectively.

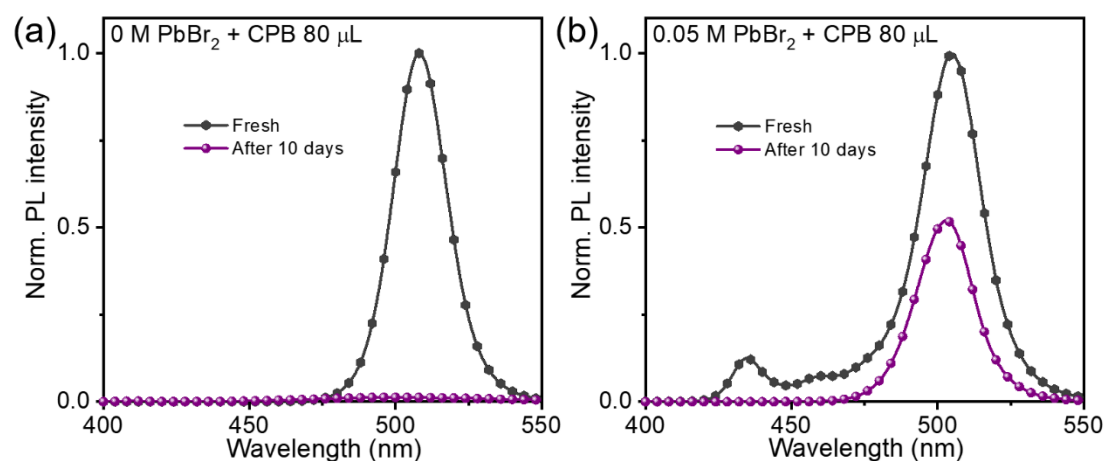


Figure S9. PL intensity changes in 10 days for nanomaterials made from (a) 0 M PbBr₂ and (b) 0.05 M PbBr₂ solution. The results demonstrated that 2D perovskite nanoplates with $n=2$ and $n=3$ synthesized using 0.25 M PbBr₂ exhibited stability, maintaining nearly the same PL intensity after ten days, compared to those synthesized with 0.1 M PbBr₂. After ten days, the PL intensity of the 2D perovskite nanoplates retained approximately 90% of the initial value. However, by day 15, a significant decrease in PL intensity was observed, indicating that the structural stability of these 2D perovskite nanoplates synthesized by our method was maintained for at least ten days. Additionally, while the nanoplates showed good photo-stability, their thermal stability was relatively lower.

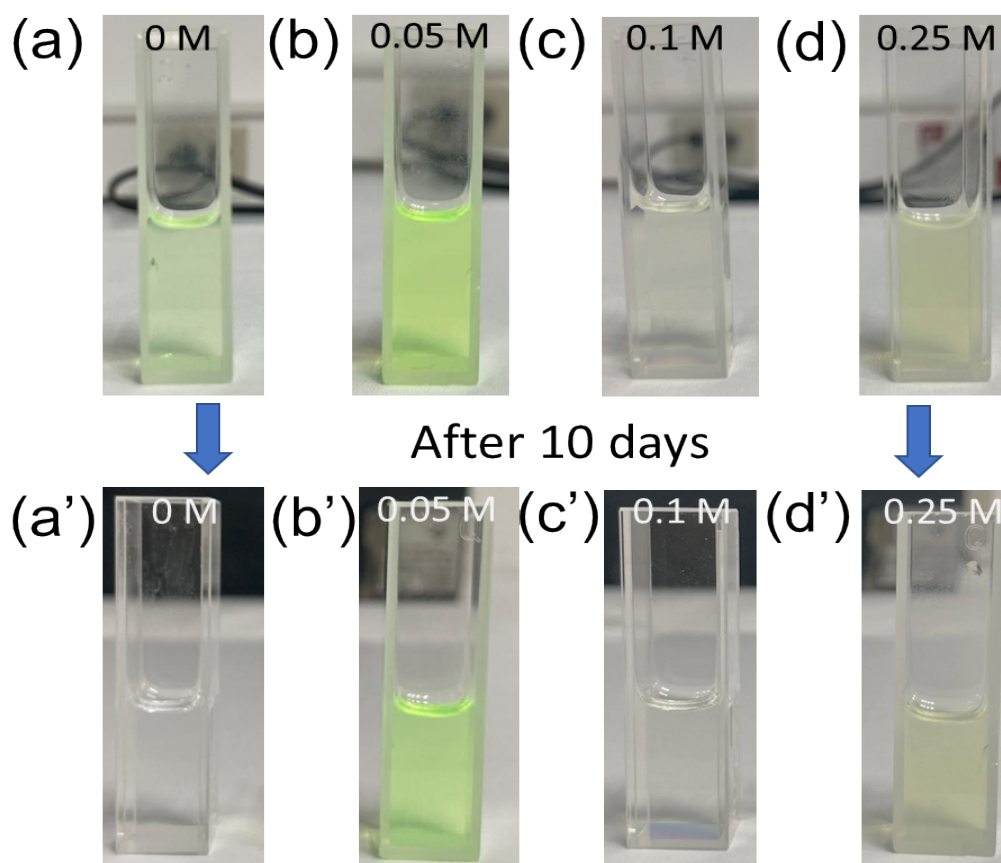


Figure S10. Pictures showing the change in color of different samples over 10 days signifying the stability of the nanomaterials in toluene for 10 days.

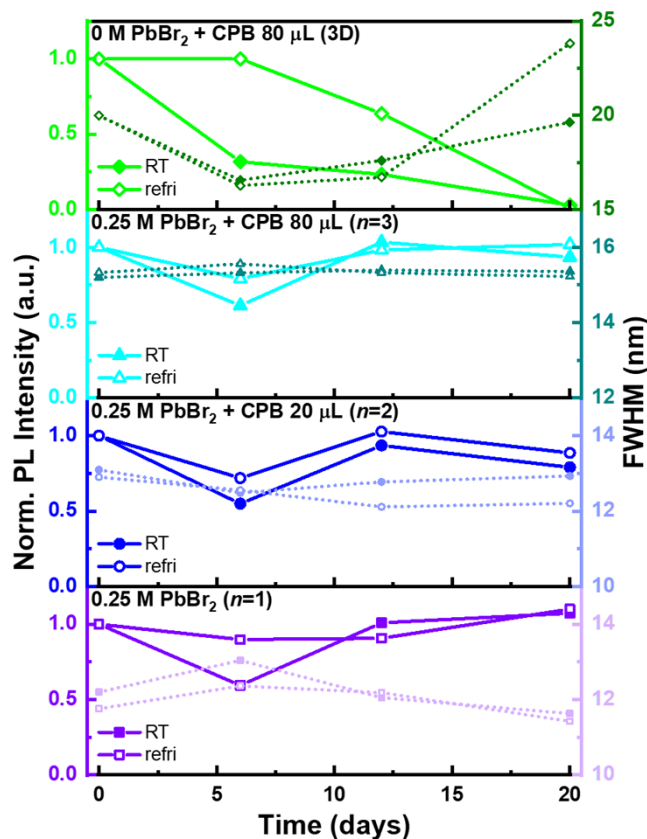


Figure S11. PL stability test of 2D ($n=1, 2, 3$) and 3D perovskite nanomaterials synthesized using a LARP method. The PL intensity of the sample solutions was monitored over time after storage under a nitrogen atmosphere at room temperature (RT) and in a refrigerator. To address the longer-term material stability, we conducted a PL stability study by storing the perovskite sample solutions under a nitrogen atmosphere at room temperature and in a refrigerator, respectively, and monitoring the changes in PL intensity over time. As shown in **Figure S11**, the 2D perovskite nanosheets ($n=1, 2, 3$) exhibited significantly better PL stability compared to the 3D perovskite nanocrystals across both storage temperatures, showing relatively minor changes in PL intensity even after 20 days. In contrast, the 3D perovskite displayed more pronounced fluctuations in PL intensity over the same period, indicating lower stability. Furthermore, an analysis of the corresponding full width at half maximum (FWHM) of the PL spectra revealed smaller variations in FWHM for the 2D samples, particularly those stored at the lower temperature. These results collectively indicate that the synthesized 2D perovskite nanosheets possess superior PL stability compared to the 3D perovskite nanocrystals under the tested storage conditions, and low-temperature storage further contributes to maintaining their material integrity, as evidenced by the more consistent spectral linewidth over the experimental period.

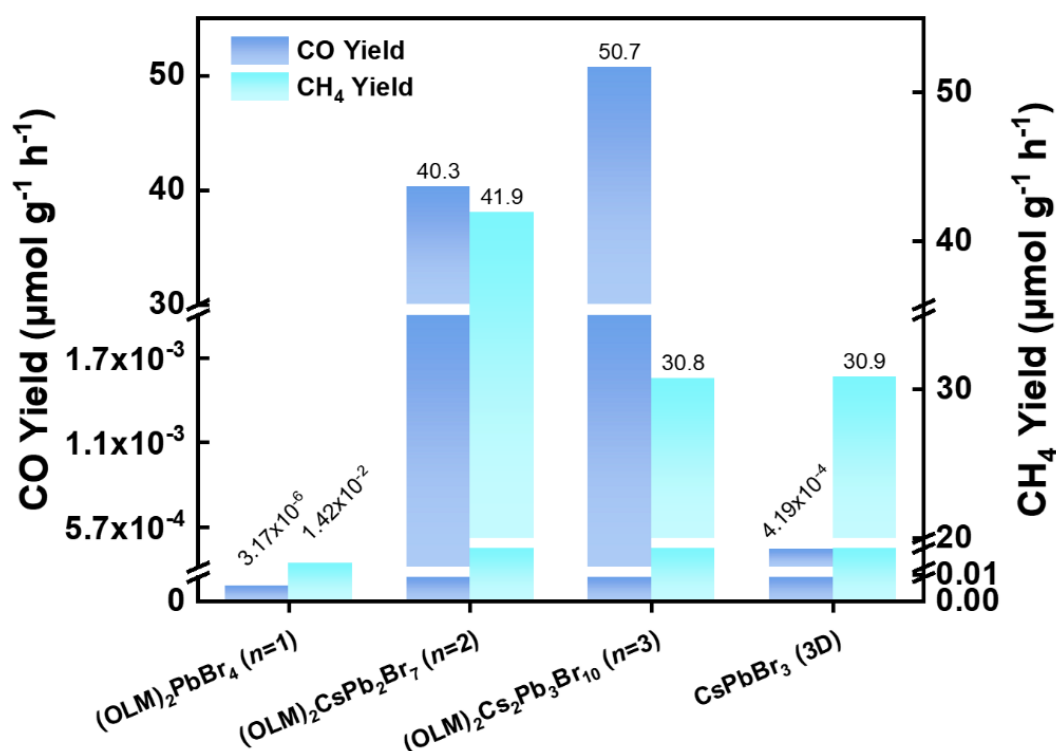


Figure S12. CO and CH₄ yields of 2D ($n=1, 2, 3$) and 3D perovskite nanomaterials in photocatalytic CO₂ reduction reactions.

To explore the potential applications of the perovskite samples in our work, their photocatalytic CO₂ reduction reaction (CO₂RR) performance was evaluated. The samples, including 2D $n=1, 2,$ and $3,$ and 3D perovskite nanomaterials, were subjected to CO₂RR under LSH 7320 LED light irradiation. The reaction products, including CO and CH₄, were subsequently analyzed using gas chromatography-mass spectrometry (GC-MS). The preliminary results revealed varying CO and CH₄ production rates among the different perovskite samples, as shown in **Figure S12**. The 2D (OLM)₂PbBr₄ ($n=1$) nanosheets exhibited a CO production rate of $3.17 \times 10^{-6} \mu\text{mol g}^{-1} \text{h}^{-1}$ and a CH₄ production rate of $1.42 \times 10^{-2} \mu\text{mol g}^{-1} \text{h}^{-1}$. The 2D (OLM)₂CsPb₂Br₇ ($n=2$) nanosheets exhibited a CO production rate of $40.3 \mu\text{mol g}^{-1} \text{h}^{-1}$ and a CH₄ production rate of $41.9 \mu\text{mol g}^{-1} \text{h}^{-1}$. The 2D (OLM)₂Cs₂Pb₃Br₁₀ ($n=3$) nanosheets demonstrated a CO production rate of $50.7 \mu\text{mol g}^{-1} \text{h}^{-1}$ and a CH₄ production rate of $30.8 \mu\text{mol g}^{-1} \text{h}^{-1}$. The 3D perovskite nanocubes exhibited a CO production rate of $4.19 \times 10^{-4} \mu\text{mol g}^{-1} \text{h}^{-1}$ and a CH₄ production rate of $30.9 \mu\text{mol g}^{-1} \text{h}^{-1}$. These findings highlight the potential of our synthesized perovskite nanomaterials as effective photocatalysts for CO₂ conversion. The observed variations in CO₂RR performance among different samples suggest that the structural and compositional modifications achieved through our synthesis method can significantly influence their catalytic activity and product selectivity. This

application example not only substantiates the novelty of our materials but also provides a compelling case for their relevance in addressing environmental challenges through CO₂ conversion.

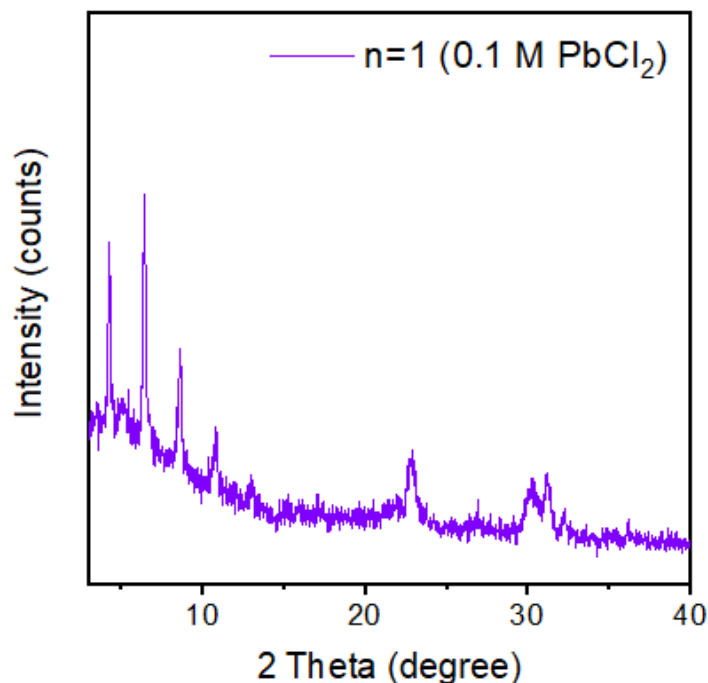


Figure S13. XRD patterns of (OLM)₂PbCl₄.

Table S1. Fitting parameters of the TRPL decay curves for 2D $n=1, 2, 3$, and 3D perovskite nanomaterials obtained using a biexponential decay model. With their respective amplitude coefficients (A_1 and A_2), the extracted lifetimes (τ_1, τ_2) represent the fast and slow decay components, respectively.

	Sample	A_1 (%)	τ_1 (ns)	A_2 (%)	τ_2 (ns)	τ_{ave} (ns)
$n=1$	0.25 M PbBr ₂	86.62	0.58	13.38	6.68	4.49
$n=2$	0.1 M PbBr ₂ + 20 μ L CPB	91.21	1.25	8.79	10.24	5.21
	0.25 M PbBr ₂ + 20 μ L CPB	88.64	1.11	11.36	10.96	6.62
$n=3$	0.1 M PbBr ₂ + 80 μ L CPB	73.87	1.06	26.13	5.98	4.34
	0.25 M PbBr ₂ + 80 μ L CPB	77.18	0.89	22.82	6.36	4.60
3D	0 M PbBr ₂ + 80 μ L CPB	27.06	2.01	72.94	16.37	15.74